

# Supplementary information for “Spatiotemporal imaging of water in operating voltage-gated ion channels reveals the slow motion of interfacial ions”

Orly B. Tarun<sup>1+</sup>, Maksim Yu. Eremchev<sup>1+</sup>, Aleksandra Radenovic<sup>2</sup>, and Sylvie Roke<sup>\*1</sup>

<sup>1</sup>Laboratory for fundamental BioPhotonics (LBP), Institute of Bioengineering (IBI), and Institute of Materials Science (IMX), School of Engineering (STI), and Lausanne Centre for Ultrafast Science (LACUS), École Polytechnique Fédérale de Lausanne (EPFL), CH-1015 Lausanne, Switzerland

<sup>2</sup>Laboratory of Nanoscale Biology, Institute of Bioengineering (IBI), School of Engineering (STI), EPFL, CH-1015 Lausanne, Switzerland

\*Corresponding author: [sylvie.roke@epfl.ch](mailto:sylvie.roke@epfl.ch)

<sup>+</sup>Equal contribution

This file includes

- S1. Sample preparation and instrumentation
- S2. Capacitance measurements of activated channels
- S3. Estimation of the number of incorporated ion channels in a lipid membrane
- S4. Second harmonic intensity changes for 500 mM and 100 mM KCl concentration

Figure S1: SH imaging setup

Figure S2: Macroscopic conductance-voltage curve of alamethicin channels

Figure S3: Time series of changes in SH intensity

## **S1. Sample preparation and instrumentation**

**Chemicals and cleaning procedures.** Alamethicin from *Trichoderma viride* (Sigma-Aldrich, >98%), 1,2-diphytanoyl-sn-glycero-3-phosphocholine (DPhPC) in powder form (>99%) (Avanti Polar Lipids, Alabama, USA), hexadecane (C<sub>16</sub>H<sub>34</sub>, 99.8%, Sigma-Aldrich), squalene (C<sub>30</sub>H<sub>50</sub>, >98%, Sigma-Aldrich), hexane (C<sub>6</sub>H<sub>14</sub>, >99%, Sigma-Aldrich), chloroform (>99.8%, Merck), hydrogen peroxide (30%, Reactolab SA), sulfuric acid (95-97%, ISO, Merck), KCl (99.999%, Aros), CaCl<sub>2</sub> (99.999%) were used as received. Aqueous solutions were made with ultra-pure water (H<sub>2</sub>O, Milli-Q UF plus, Millipore, Inc., electrical resistance of 18.2 MΩ cm). All aqueous solutions were filtered with 0.1 μM Millex filters. The coverslips used in the imaging were pre-cleaned with piranha solution (1:3 - 30% H<sub>2</sub>O<sub>2</sub>: 95-97% H<sub>2</sub>SO<sub>4</sub>) and thoroughly rinsed with ultrapure water. The chamber and Teflon films that were used in forming freestanding planar lipid bilayers were cleaned with ethanol, methanol, and chloroform and thoroughly rinsed with ultrapure water.

### **Formation of freestanding lipid bilayers and incorporation of alamethicin peptides.**

Freestanding horizontal planar lipid bilayers were formed following the procedure of Montal-Müller<sup>1,2</sup>. Two separated lipid monolayers on an air/water interface were apposed in a ~80-100-μm aperture in 25-μm thick Teflon film. Condensed lipid monolayers were formed on an air/water interface by depositing 3-8 μL of 10 mg/mL lipid solution in chloroform<sup>3</sup>. Prior to forming a bilayer, the Teflon film was pre-painted on both sides with 1 μL of 99.5:0.5 vol% mixtures of hexane and an alkane solvent (squalene or hexadecane). We waited at least 10 minutes for the pre-painting solution to evaporate (hexane evaporates, alkane solvent remains). After bilayer formation, the Teflon film that contains the bilayer was positioned horizontally for imaging as shown in Fig. 1B. The presence of a bilayer was confirmed with white light imaging and electrical recordings. Capacitance and resistance measurements were taken with a HEKA patch clamp amplifiers. Capacitance measurements were made with HEKA's built-in software based lock-in amplifier<sup>4</sup>. Only bilayers with specific capacitance,  $C_m > 0.7 \mu\text{F}/\text{cm}^2$  and specific resistance,  $R_m \sim 10^8 \Omega \cdot \text{cm}^2$ <sup>5,6</sup> are used.

To incorporate alamethicin ion channels, we added 5 μL of alamethicin peptide solution (in absolute ethanol with a concentration of 9.8 μg/mL). The corresponding concentration of alamethicin in solution is ~50 nM (or 98 ng/mL), the top compartment having 500 μL of aqueous solution. Unless otherwise stated, we added peptides on the top compartment (see Fig. 1B). The bottom compartment was the electrical ground of the system. Incorporation of voltage-gated alamethicin peptides was confirmed by performing current – voltage (I-V) curves by

ramping the voltage from -200 mV to 200 mV. Typical IV curves show a voltage threshold where the current exponentially jumps as shown in Fig. 1C.

### Second Harmonic (SH) imaging experiments.

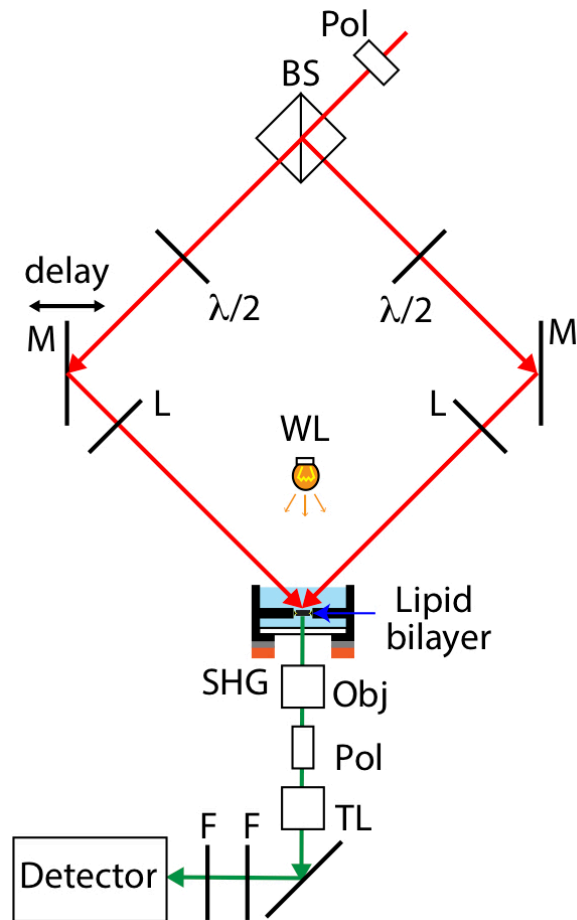


**Figure S1: SH imaging setup.** Two near-IR 190-fs 200-kHz pulsed laser beams are incident on the lipid membranes. SH photons are detected in the phase-matched direction. The beams are polarized in the plane of incidence (P). The sample chamber is not to scale. BS: beam splitter; F: filter; L: lens; M: mirror; Obj: objective lens; Pol: linear polarizer; TL: tube lens; WL: white-light source;  $\lambda/2$ : half-wave plate.

The second harmonic (SH) imaging setup has been previously characterized in detail, see refs.<sup>7-9</sup>. In brief, two counter propagating beams (pulse duration of 190 fs, wavelength of 1030 nm and repetition rate of 200 KHz from a Yb:KGW femtosecond laser, (Light Conversion Ltd.)) were incident at  $45^\circ$  with respect to the surface normal (Fig S1, Fig. 1B). The beams were loosely focused using a  $f=20$  cm doublet lens (B coating, Thorlabs). The phase-matched SH photons were collected with a 50x objective lens (Mitutoyo Plan Apo NIR HR Infinity-Corrected Objective, 0.65 NA in combination with a tube lens (Mitutoyo MT-L), a 900 nm short pass filter

(FES0900, Thorlabs), a 515 nm band pass filter (FL514.5-10) and an intensified electronically amplified CCD camera (IE-CCD, PiMax4, Princeton Instruments). A 400 mm meniscus lens was placed behind the objective lens to remove spherical aberrations induced by the coverslip. The transverse resolution was 430 nm. All images were recorded with the beams polarized parallel to the plane of incidence (P). For white-light imaging, the sample is illuminated from the top using a white light source and the linear scattered light is detected in the forward direction with the same objective lens (Fig. S1).

## S2. Capacitance measurements of activated channels

To measure the membrane capacitance of operating ion channels, we used the "SINE + DC" lock-in mode of HEKA patch clamp amplifiers. Briefly, we used a stimulus ( $U$ ) with an AC excitation  $U_1$  and a DC bias  $U_0$ ,

$$U = U_0 + U_1 \sin 2\pi ft$$

where  $U_0 = 1$  mV for close channels and  $U_0 > 100$  mV for open channels (depending on the voltage threshold needed to open the channels, we set  $U_0$  to be 20-30 mV above the threshold),  $U_1 = 10$  mV,  $f = 1$  kHz and  $t = 100$  ms, corresponding to 100 sine wave cycles. We obtained capacitance measurement every 200 ms while the channels are opened or closed by setting  $U_0$  to a block square pulse stimulus (see Fig. 2B).

## S3. Estimation of the number of incorporated ion channels in a lipid membrane

Figure S2 shows the macroscopic conductance – voltage ( $G$ - $V$ ; with  $G=I/V$ ) curve. The red line represents an exponential fit that is common for alamethicin ion channels<sup>10,11</sup>. Macroscopic conductance ( $G$ ) curves can be used to estimate the number of open ion channels ( $N$ ), provided the single channel conductance  $\bar{\gamma}$  is known. Assuming  $\bar{\gamma}$  does not depend on  $V$  we have  $G(V) = N(V)\bar{\gamma}$ . For the single ion channel conductance, we rely on a study<sup>12</sup>, where the current through single pores was measured. In Ref.<sup>12</sup> the average single channel conductance was determined for alamethicin in a bilayer composed of phosphatidyl ethanolamine (PE) lipids, and with two different salt concentration: for 1 M NaCl solution, and  $0.6 \cdot 10^{-7}$  g/mL total alamethicin concentration,  $\bar{\gamma} = 2.5 \cdot 10^{-9}$  S and for 0.05 M NaCl solution,  $2.0 \cdot 10^{-6}$  g/mL,  $\bar{\gamma} = 2.08 \cdot 10^{-10}$  S. Interpolating between these two single conductance values, at 0.5 M salt concentration, we get  $\bar{\gamma} = 1.3 \cdot 10^{-9}$  S. Using this number, we obtain the values displayed on the right axis of Fig. S2. For a 200 mV potential difference, the total number of open ion channels is  $6.5 \cdot 10^7$  and given a

membrane with diameter of  $\sim 100 \mu\text{m}$ , the average area per ion channel is  $\sim 120 \text{ nm}^2$ , meaning there are on average  $\sim 1500$  opened ion channels per pixel ( $430 \text{ nm} \times 430 \text{ nm}$ ).

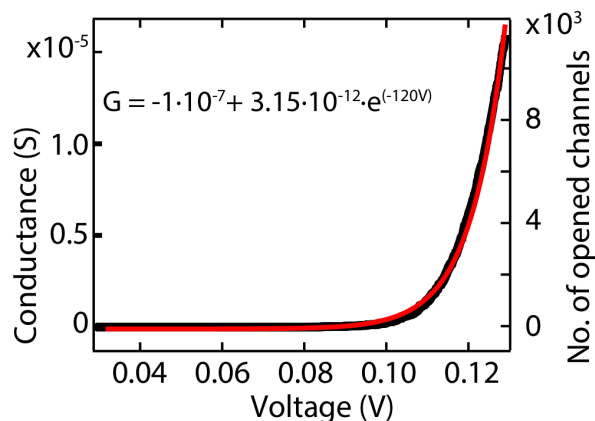


**Figure S2: Macroscopic conductance-voltage curve of alamethicin channel in 500 mM KCl.** The conductance was derived from the positive stimulus of Fig. 1B. Data points (black) are fitted with an exponential curve (solid red line). The right axis shows the calculated number of opened channels using the average single pore conductance from Ref <sup>12</sup> (1.3 nS per channel).

#### **S4. Second harmonic intensity changes for 500 mM and 100 mM KCl concentration**

Figure S3A shows the time series of the integrated SH intensity over the whole image for a sequence of activation and deactivation cycles. The experimental configuration, the composition of the bilayer and the amount of added alamethicin is the same as Fig. 2A. The only difference is the ionic strength of the solution at 500 mM KCl. Black dots are data points, red and blue curves represent exponential fits for the activation and deactivation cycles correspondingly. The stimulus (green curve) indicates the timing when the external field of 200 mV was applied. We compared the time constants in Fig. S3A (500 mM KCl) with those of Fig. 2A (100 mM KCl). Figure S3B and S3C shows the corresponding activation/deactivation time constants as a function of activation/deactivation cycles for 500 and 100 mM KCl solution. It can be seen that the time constants obtained for 500 mM solution are higher than time constant for 100 mM solution, suggesting that relaxation processes are faster for low ionic strength solutions.

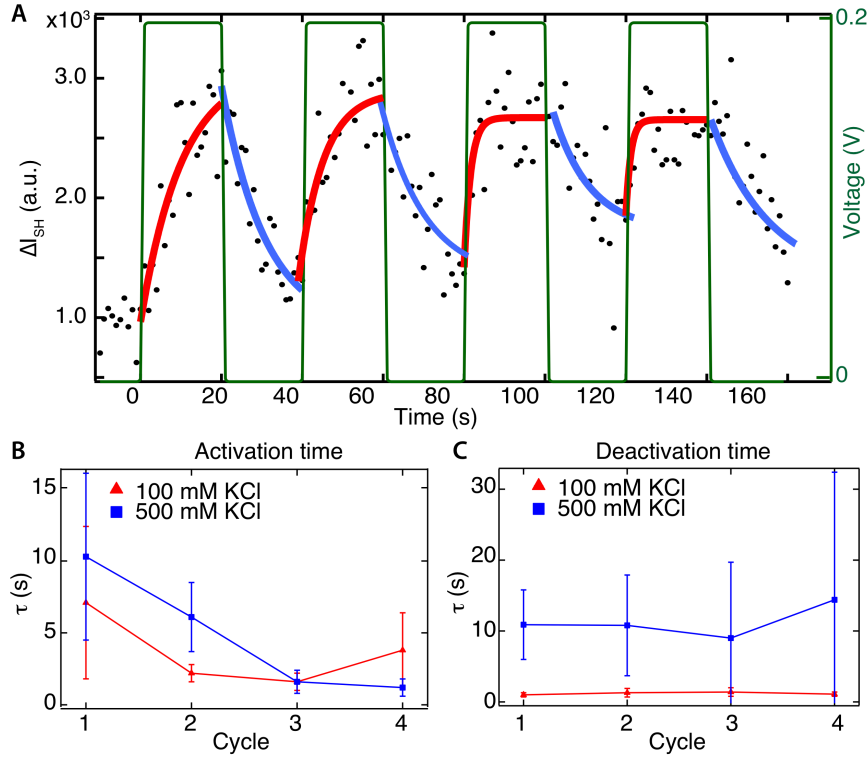


**Figure S3: Time series of changes in second harmonic (SH) intensity.** (A) Time series of SH intensity (left axis) following the activation and deactivation of alamethicin channels (500 mM KCl, 0.1  $\mu\text{g}/\text{mL}$  alamethicin added to one side of the bilayer). The 20 s stimulus (green curve) indicates the timing when the channels are activated (200 mV) and when the channels are deactivated (0 mV). Each data point (black dot) represent the spatially averaged SH intensity (500 ms acquisition time) of the membrane. The data points in each activation and deactivation steps are piece-wise fitted with an exponential curve ( $y_0 + Ae^{(t-t_0)/\tau}$ ), where  $\tau$  is the time constant,  $y_0$  the offset and  $A$  the magnitude. Red solid curves are exponential fits for activation steps while blue solid curves are exponential fits for deactivation steps. Time constants for the activation (B) and deactivation (C) cycles obtained from exponential fits at different ionic strengths (red – 100 mM, blue – 500 mM KCl).

## References

- 1 Montal, M. & Mueller, P. Formation of bimolecular membranes from lipid monolayers and a study of their electrical properties. *Proceedings of the National Academy of Sciences of the United States of America* **69**, 3561-3566, doi:10.1073/pnas.69.12.3561 (1972).
- 2 Alvarez, O. & Latorre, R. Voltage-dependent capacitance in lipid bilayers made from monolayers. *Biophysical journal* **21**, 1-17, doi:10.1016/S0006-3495(78)85505-2 (1978).
- 3 Roke, S., Schins, J., Müller, M. & Bonn, M. Vibrational Spectroscopic Investigation of the Phase Diagram of a Biomimetic Lipid Monolayer. *Phys. Rev. Lett.* **90**, 128101-128101, doi:10.1103/PhysRevLett.90.128101 (2003).
- 4 Elektronik, H. & Gmbh, S. Tutorial. **49**, 1-48.
- 5 Horner, A., Akimov, S. A. & Pohl, P. Long and Short Lipid Molecules Experience the Same Interleaflet Drag in Lipid Bilayers. *Physical Review Letters* **110**, 268101 (2013).

- 6 Gutsman, T., Heimburg, T., Keyser, U., Mahendran, K. R. & Winterhalter, M. Protein reconstitution into freestanding planar lipid membranes for electrophysiological characterization. *Nature Protocols* **10**, 188-198, doi:10.1038/nprot.2015.003 (2014).
- 7 Macias-Romero, C. *et al.* High throughput second harmonic imaging for label-free biological applications. *Optics express* **22**, 31102-31112, doi:10.1364/OE.22.031102 (2014).
- 8 Mondal, P. P. Temporal resolution in fluorescence imaging. *Frontiers in Molecular Biosciences* **1**, 11, doi:10.3389/fmolb.2014.00011 (2014).
- 9 Macias-Romero, C. *et al.* Probing rotational and translational diffusion of nanodoublets in living cells on microsecond time scales. *Nano Lett.* **14**, 2552-2557, doi:10.1021/nl500356u (2014).
- 10 Hall, J. E., Vodyanoy, I., Balasubramanian, T. M. & Marshall, G. R. Alamethicin. A rich model for channel behavior. *Biophysical Journal* **45**, 233-247, doi:https://doi.org/10.1016/S0006-3495(84)84151-X (1984).
- 11 Cafiso, D. S. Alamethicin: A Peptide Model for Voltage Gating and Protein-Membrane Interactions. *Annual Review of Biophysics and Biomolecular Structure* **23**, 141-165, doi:10.1146/annurev.bb.23.060194.001041 (1994).
- 12 Eisenberg, M., Hall, J. E. & Mead, C. A. The nature of the voltage-dependent conductance induced by alamethicin in black lipid membranes. *The Journal of Membrane Biology* **14**, 143-176, doi:10.1007/BF01868075 (1973).